ANL/ET/CP--85172
CONF-9504156--2

Degradation of Structural Ceramics by Erosion*

J. L. Routbort
Energy Technology Division
Argonne National Laboratory
Argonne, IL 60439–4838

December 1994

The submitted manuscript has been authored by a contractor of the U.S. Government under contract No. W-31-109-ENG-38. Accordingly, the U.S. Government retains a nonexclusive, royalty-free license to publish or reproduce the published form of this contribution, or allow others to do so, for U.S. Government purposes.

DISCLAIMER

This report was prepared as an account of work sponsored by an agency of the United States Government. Neither the United States Government nor any agency thereof, nor any of their employees, makes any warranty, express or implied, or assumes any legal liability or responsibility for the accuracy, completeness, or usefulness of any information, apparatus, product, or process disclosed, or represents that its use would not infringe privately owned rights. Reference herein to any specific commercial product, process, or service by trade name, trademark, manufacturer, or otherwise does not necessarily constitute or imply its endorsement, recommendation, or favoring by the United States Government or any agency thereof. The views and opinions of authors expressed herein do not necessarily state or reflect those of the United States Government or any agency thereof.

This INVITED manuscript is to be presented to a Research Assistance Task Force sponsored by DOE, EPRI, and NIST, Charlotte, North Carolina, April 10-12, 1995. Proceedings to be published in the Journal of Nondestructive Evaluation

*This work was supported by the U.S. Department of Energy under Contract W–31–109–ENG–38.

MASTER

DISTRIBUTION OF THIS DOCUMENT IS UNLIMITED 85

Degradation of Structural Ceramics by Erosion

J. L. Routbort

Energy Technology Division, Argonne National Laboratory, Argonne, Illinois 60439–4838

ABSTRACT

Materials wastage by solid-particle erosion can be severe and can limit lifetimes. This paper will review the theoretical description of solid-particle erosion in brittle materials, which is well-developed for monolithic ceramics. The models can usually account for effects from the principal projectile properties of size, impact velocity, and impact angle. Materials parameters such as fracture toughness and hardness can be included. Steady-state erosion measurements on a wide variety of ceramics, ranging from Si single crystals to SiC–whisker-reinforced Al_2O_3, are reviewed and compared with the models. It is believed that R-curve behavior and/or particle fragmentation is responsible for discrepancies between theory and experimental results for composite ceramics. In addition, the theories make no attempt to describe threshold or incubation effects.

I. INTRODUCTION

Lifetime predictions of materials subjected to solid-particle erosion depend on exact knowledge of the particle flow, specifically, distributions of erodent velocities, sizes, shapes, and impact angles. In addition, the erodent material and its flux must be determined. These aspects of solid-particle erosion, while important, are usually determined from flow models, and are not the focus of this article. Also, erosive damage of a brittle solid will affect its strength, which could play an important role in lifetime predictions. This issue will not be considered. The objective of this paper is to review the other essential component for predicting lifetimes, namely, an accurate, physically based description of the erosion process in terms of both the erodent properties, assumed given, and the target properties. It will be shown that further work on structural ceramics is needed before a reliable model can be developed to accurately predict lifetimes.

Most aspects of erosion of brittle solids have been recently reviewed [1]. It is generally accepted that material degradation resulting from the impact of an angular erodent occurs by formation and propagation of lateral cracks on the surface under the driving forces imposed by particle–impact events [2]. Contact conditions of the erodent play a role, but both dynamic [2] and quasi-static [3] models of erosion predict that the steady-state erosion rate, ΔW (amount of target removed for amount of abrasive hitting the target in units of g/g), is proportional to a power law of the form

$$\Delta W \propto V^{n} D^{2/3} \rho^{p} (K_{IC})^{-4/3} H^{q}, \qquad (1)$$

where V, D, and ρ are the impacting particle velocity, mean diameter, and density, respectively. The target materials parameters are the fracture toughness K_{IC} and the hardness H. Static K_{IC} and H are used, because of lack of information on the dynamic values. It is extremely important to note that Eq. 1 is based on the accumulation of single–impact events, whereas the situation in an actual application is much more complex. The equation does not consider possible threshold effects, which could be based on the minimum energy needed to nucleate a lateral crack.

The constant of proportionality has not been investigated but can depend on the contact model used. In general, the velocity exponent n varies between ≈ 2.0 and 3.2, depending on erodent shape and contact conditions. The density exponent is ≈ 1.2. The dependence on H is weak, with the exponent varying between -0.24 and 0.11. Therefore, it is expected that, under a given set of erosive conditions, constant velocity and impact angle, the materials parameter K_{IC} will have the largest effect on erosion resistance.

Fracture toughness of monolithic ceramics can be significantly enhanced by addition of ceramic whiskers. Models of the improvement in toughness discuss fiber sliding, crack deflection, crack bowing, and/or microcrack formation [4]. Enhanced toughening from whisker additions has been observed in Al_2O_3 [5], Si_3N_4 [6], toughened ZrO_2 [7], $MoSi_2$ [8], and magnesia-alumina spinels [9]. Indeed, Becher and Wei [5] have shown that the K_{IC} of Al_2O_3 can be doubled by adding 20 vol.% SiC whiskers. Generally, however, the toughness in these materials is not a constant but is a function of crack length, R–curve, or crack resistance–versus –crack–length behavior.

Toughening can also be accomplished by microstructural manipulation: an example being an in–situ–reinforced Si_3N_4. This material exhibits a pronounced R–curve, but the long-crack-length-limit fracture toughness is $\approx$

50% higher than that of an equivalent fine-grained Si_3N_4 [10]. The increased toughness should result in enhanced erosion resistance and, therefore, possible applications for these hard, new materials are ones in which the materials are subjected to erosion by solid particles, e.g., pump vanes, fuel regulators for jet engines, cutting tools, etc.

A reasonably large solid-particle erosion data base for structural ceramics exists. Some materials investigated include Al_2O_3-SiC(w) (where (w) denotes whisker) [11, 12], Si_3N_4-SiC(w) [13,14], Si_3N_4-Si_3N_4(w), and Y_2O_3-stabilized ZrO_2 (TZ3Y)-Al_2O_3(w) composite [15]. Recently [10], erosion and R–curve results have been reported on in–situ–reinforced Si_3N_4 and an equivalent fine-grained Si_3N_4. The effect of erosion damage on the strength in an in–situ–reinforced Si_3N_4 has also been reported [16].

This paper will review some of the erosion results for various modern structural ceramics. Trends in the behavior of the steady-state erosion rates with the principal variables (V and K_{IC}) will be compared with theoretical predictions. Failure of the models for materials exhibiting pronounced R-curve behavior will be discussed. Finally, further experimental/theoretical work will be suggested to improve component lifetime predictions.

II. EXPERIMENTAL PROCEDURES

Measurements of solid-particle erosion with basic research objectives are usually performed under well-defined impact conditions, i.e., the impact angles, velocities, and erodent size and materials are carefully controlled. In addition, the flux rate is varied so that particle–particle interactions in the impacting stream can be neglected. Two general types of apparatus are used in these experiments: a gas gun, in which the particles are carried by the gas, and a slinger-type apparatus [17]. The latter experiments are performed in a vacuum and have a narrow velocity distribution, but the impact angle varies across the specimen. On the other hand, in the gas gun experiments, the velocities of the particles depend particle size, and the flow pattern is disturbed at the stagnation point. Velocities of impact can be conveniently varied between 10 and 150 m/s and angular SiC or Al_2O_3 abrasives with mean diameters from 40-1000 μm are commercially available. The effect on erosion of the ratio of the erodent hardness to that of the target has been discussed [14, 18, 19]. The angle of incidence is usually between 15 and 90°, but this paper will concentrate on results obtained at normal incidence.

III. RESULTS AND DISCUSSION

Figure. 1 presents typical erosion data measured for Al_2O_3, Si_3N_4, Al_2O_3 + SiC(w), and Si_3N_4 + Si_3N_4(w) at normal incidence, 100 m/s, and with 42–μm–diameter SiC abrasives. After an initial transient, the slope of the weight loss versus the dose that is impacting the sample becomes constant and is, by definition, equal to the steady-state erosion rate. The transient, despite its potential importance in modeling materials degradation, has never been investigated. It is likely that the transient is the result of incubation effects. That is, there is a minimum amount of kinetic energy that must be transferred to the sample to develop a subsurface crack network necessary to sustain the steady state. This might correspond to unit coverage of the target; a fluence such that the contact areas of each impact overlap. Generally, for a brittle material, the contact areas are ≈ 1/10 the projected area of an angular projectile.

Also, it is clear that threshold effects can exist. Low–velocity impacts may not result in nucleation of lateral cracks because they cannot supply a kinetic energy larger than the energy necessary to nucleate a crack. There is some evidence for the existence of threshold effects in single–crystal Si [20]. In this case, the steady-state equation was modified to include a threshold velocity V_o and erodent particle size D_o to give

$$\Delta W \propto (V-V_o)^n (D-D_o)^{2/3} \rho^p (K_{IC})^{-4/3} H^q. \quad (2)$$

However, threshold experiments are very difficult to perform, requiring low velocities and/or small particle sizes, and no experimental results on thresholds effects in a brittle solid, except Si single crystals, have been reported.

Threshold and incubation effects could have important ramifications on predictions of lifetimes. If in–service fluences and/or particle velocities or sizes are low enough, erosion may not be a problem. Fortunately, a steady–state erosion model would, in all cases, overestimate the amount of materials wastage.

Steady-state erosion rates obtained from the slopes of data like that shown in Fig. 1, measured with 143–μm–diameter SiC abrasives impacting an Al_2O_3-SiC (w) composite, are presented in Fig. 2. The velocity dependence of ΔW can indeed be described by a power law, as predicted by the models. The velocity exponents n at normal incidence are tabulated in Table 1 for a variety of composites with two types of erodents. It should be noted that microstructura; affects erosion rate. That is, ΔW of various types of Al_2O_3 varies by a factor of ≈ 5 when erosion occurs under identical conditions (Fig. 3) [21]. These differences are probably related to the ratio of grain size to impact size and to the amount and type of glassy phase at the grain boundaries. It turns out that even anodized aluminum erodes at the same rate as most bulk Al_2O_3. Therefore, if a metal simultaneously undergoes oxidation and erosion, the behavior can be predicted from knowledge of ΔW of the base oxide, if the oxidation rate is higher than the erosion rate.

Table 1 indicates that there is a wide discrepancy between n values obtained for the softer Al_2O_3 than for the harder SiC abrasive. The explanation lies in the fact that the composites can be harder than the erodent [14, 18, 19] and considerable energy is expended in fracture and blunting of the impacting particle, energy which is unavailable for nucleation and propagation of lateral cracks that control erosion. Larger particles fragment more than smaller particles [15] although even hard SiC erodents fragment [18]. For the harder erodents, the n values are, for the most part, in accord with the theoretical predictions and comparable to those measured for monolithic ceramics [1]. Erodent fragmentation is therefore a significant problem that must be described before an accurate model to predict lifetimes can be developed.

Softer particles remove material less efficiently than do harder particles. Figure 4 illustrates that ΔW can differ by a least an order of magnitude [19] depending on the erodent. Photomicrographs obtained by scanning electron microscopy show that, on surfaces eroded by softer erodents particle, crushing occurred, and that some of the crushed erodent adhered to the impact site. The surface of the composite eroded by the harder material has sharper features and contains more cracks. Only the rate of material removal changed; the mechanism appeared to be the same. Scattergood et al. [18, 21] concluded from a series of experiments with different Al_2O_3 targets, that for the softer erodents, more damage accumulation is necessary to build up requisite stresses to produce lateral cracks. This confirms that the incubation depends on the properties of the erodent as well as the target, consistent with physical intuition.

The dependence of ΔW on K_{IC}, as shown in Fig. 5, is not predicted by the existing model. The predicted slope of -4/3, as shown by the solid line, fits the experimental results for the Al_2O_3-SiC(w) composite, but not for the other composites. For the other composites, increases in erosion resistance have been offset by changes that are detrimental to erosion. For example, the increase in toughness in the Si_3N_4-SiC(w) system is believed to be due to microcracking caused by the presence of a grain boundary glass phase [6] which, while increasing K_{IC}, would help propagate the lateral cracks responsible for erosion [22]. Therefore, not all toughening processes decrease ΔW and the models must be applied with caution.

Srinivasan and Scattergood [22] investigated a series of partially stabilized zirconias. They showed that ΔW is not proportional to $(K_{IC})^{-4/3}$ and invoked the explanation that the correct toughness is that value relevant for the size scale of the erosion–impact events K^{op}. The latter can be significantly less than the maximum toughness. They found a good correlation between ΔW and K^{op}, which was determined from the intersection of the stress– intensity factor and the crack–driving force. Recent measurements on a fine-grained and an in-situ–reinforced Si_3N_4, despite the differences in the R–curve behavior, show that ΔW is nearly independent of the material. This was interpreted as being due to the fact that the toughness for erosion is determined by crack initiation and is consistent with the K^{op} concept. Nevertheless, it should be pointed out that, in these tough, hard composites, the operative toughness is that determined for short crack lengths, and it is precisely that region of the R-curve which is not very experimentally accessible.

IV. CONCLUSIONS

Lifetime predictions based on first–principle solid–particle erosion models developed for monolithic brittle materials must be modified to describe the behavior of structural ceramics. The models fail to account for threshold and incubation effects or particle fragmentation. R–curve behavior and an operative toughness are also important considerations. Little experimental or theoretical work on these topics exists. Therefore, if accurate lifetime predictions are required, these topics, despite the considerable experimental problems, must be systematically investigated and understood.

ACKNOWLEDGMENTS

The author is grateful to the many students and colleagues who have contributed to this work over the last decade. This work was supported by the U.S. Department of Energy under Contract W–31–109–ENG–38.

REFERENCES

[1] J. L. Routbort and R. O. Scattergood, in Erosion of Ceramic Materials, J. E. Ritter, ed., Trans Tech Publication, Switzerland (1992), pp. 23-51.

[2] A. G. Evans, M. E. Gulden, and M. E. Rosenblatt, Proc. Royal Soc. London, Ser. A361, 343-365 (1979).

[3] S. M. Wiederhorn and B. R. Lawn, J. Am. Ceram. Soc. 62, 66-70 (1979).

[4] R. W. Rice, Ceram. Eng. Sci. Proc. 2, 661-701 (1981).

[5] P. F. Becher and G. C. Wei, J. Am. Ceram. Soc. 67, C267-269 (1984).

[6] J. P. Singh, K. C. Goretta, D.S. Kupperman, and J.L. Routbort, Adv. Ceram. Mater. 3, 357-360 (1988).

[7] N. Claussen and G. Petzow, Tailoring of Multiphase and Composite Ceramics, Plenum Publishing Corp., New York (1986), pp. 649-662.

[8] F. D. Gac and J.J. Petrovic, J. Am. Ceram. Soc. 68, C200-201 (1985).

[9] P. C. Panda and E. R. Seydel, Am. Ceram. Soc. Bull. 65, 338-341 (1986).

[10] M. Marrero, J. L. Routbort, P. Whalen, C.-W. Li, and K. R. Karasek, Wear, 162-164, 280-284 (1993).

[11] M. T. Sykes, R. O. Scattergood, and J. L. Routbort, Composites 18, 153-163 (1987).

[12] S. Wada, N. Watanabe and T. Tam, J. Ceram. Soc. Jpn. Int. Ed. 96, 113-119 (1988).

[13] C. T. Morrison, J. L. Routbort, and R. O. Scattergood, Mater. Res. Soc. Symp. Proc. 78, 207-214 (1987).

[14] S. Wada, N. Watanabe, T. Tani and O. Kamigaito, in Structural Ceramics, Fracture Mechanics, Vol. 5, M. Doyama, S. Somiya and R. Chang, eds., Mater. Res. Soc., Pittsburg, PA (1989), pp. 481-490.

[15] J. L. Routbort, D. A. Helberg, and K. C. Goretta, J. Hard Mater. 1, 123-135 (1990).

[16] J. E. Ritter, S. R. Choi, K. Jankus, P. J. Whalen, and R. G. Rateick, J. Mater. Sci. 26, 5543-5546 (1991).

[17] T. H. Kosel, R. O. Scattergood, and A. P. L. Turner, Wear of Materials, ASME, New York, (1979), pp. 192-204.

[18] S. Srinivasan and R. O. Scattergood, Wear 128, 139-52 (1988).

[19] J. L. Routbort, C.-Y. Chu, J. M. Roberts, J. P. Singh, W. Wu and K. C. Goretta, Proceedings Corrosion-Erosion-Wear of Materials at Elevated Temperatures, A.V. Levy, ed., National Assoc. of Corrosion Engrs., Houston, TX (1991), pp. 31-1-31-9.

[20] D. B. Marshall, A. G. Evans, M. E. Gulden, J. L. Routbort, and R. O. Scattergood, Wear 71, 363-373 (1981).

[21] L. M. Murugesh and R. O. Scattergood, J. Mater. Sci. 26, 5456-5466 (1991).

[22] J. L. Routbort, K. C. Goretta, C.-Y. Chu, and J. P. Singh, in Tribology of Composite Materials, P. K. Rohatgi, P. J. Blau, and C. S. Yust, eds., ASM, Materials Park, OH (1990), pp. 355-360.

[22] S. Srinivasan and R. O. Scattergood, Adv. Ceram. Mater. 3, 345-352 (1988).

Figure Captions

Figure 1. Weight loss versus erodent dose for 42 μm diameter SiC particles impacting at normal incidence at 100 m/s for Al_2O_3 (open squares), Al_2O_3-25 wt.% SiC(w) (open triangles), Si_3N_4 (filled squares), and Si_3N_4-15 vol.% Si_3N_4(w) (filled triangles).

Figure 2. Steady-state erosion rates at normal incidence for a series of Al_2O_3-SiC(w) composites with 143–μm–diameter SiC erodents. Weight percent of whiskers of each composite is: open circles–0, open squares–5, open triangles–15, and solid circles–25.

Figure 3. Steady-state erosion rates for various grades of alumina measured for 405–μm Al_2O_3 erodents impacting at normal incidence [21].

Figure 4. Steady-state erosion rate measured at normal incidence for impacting velocity of 100 m/s with 143–μm–diameter erodents of SiC (circles), Al_2O_3 (squares), and a 75% Al_2O_3 - 25% ZrO_2 abrasive (triangles).

Figure 5. Steady-state erosion rate versus $1/K_{IC}$ for four whisker-reinforced composites measured with 143–μm–diameter SiC abrasives. Symbols are Si_3N_4 (squares), Al_2O_3–SiC(w) (open circles), Si_3N_4–SiC(w) (filled circles), and Y_2O_3–stabilized ZrO_2–Al_2O_3(w) (triangles).

Table I. Values of velocity exponent n in $\Delta W \propto V^n$, measured for various structural ceramics at normal incidence with SiC and Al_2O_3 erodents

Material	Velocity [m/s]	n 143 µm-SiC	n 143 µm-Al_2O_3	References
Al_2O_3	40-100	2.3	2.3	11,15
Al_2O_3-5% SiC(w)	40-100	2.5	1.7	11,15
Al_2O_3-15% SiC(w)	40-100	2.1	0.7	11,15
Al_2O_3-25% SiC(w)	40-100	2.0	1.1	11,15
Si_3N_4	40-100	2.7	–	15
Si_3N_4-5% Si_3N_4(w)	40-100	2.6	–	15
Si_3N_4-15% Si_3N_4(w)	40-100	2.8	–	15
TZ3Y	40-100	2.8	–	15
TZ3Y-15% Al_2O_3(w)	40-100	2.8	–	15
TZ3Y-25% Al_2O_3(w)	40-100	2.7	–	15
Si_3N_4	80-140	–	2.6*	13
Si_3N_4-10v % Si_3N_4(w)	80-140	–	2.4*	13
Si_3N_4-20 v% Si_3N_4(w)	80-140	–	2.2*	13
Si_3N_4-fine grain	50-100	2.4	–	10
Si_3N_4-in situ	50-100	2.1	–	10

*Measured with 63–µm–diameter erodents

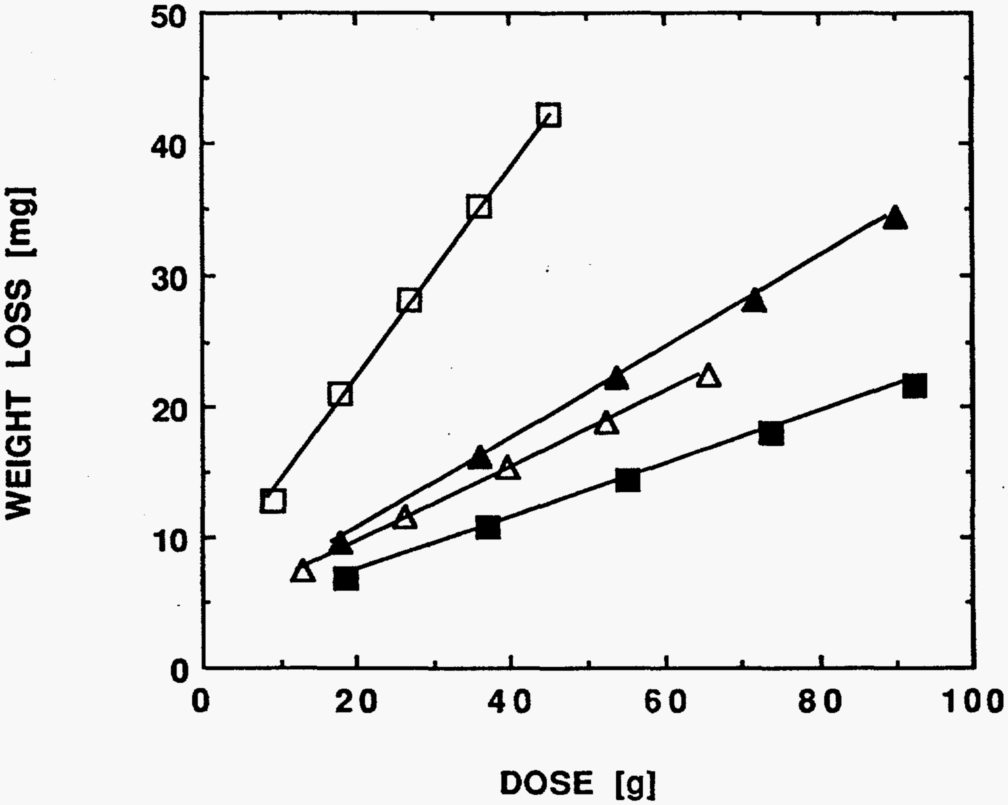

Figure 1. Weight loss versus erodent dose for 42 μm diameter SiC particles impacting at normal incidence at 100 m/s for Al_2O_3 (open squares), Al_2O_3-25 wt.% SiC(w) (open triangles), Si_3N_4 (filled squares), and Si_3N_4-15 vol.% Si_3N_4(w) (filled triangles).

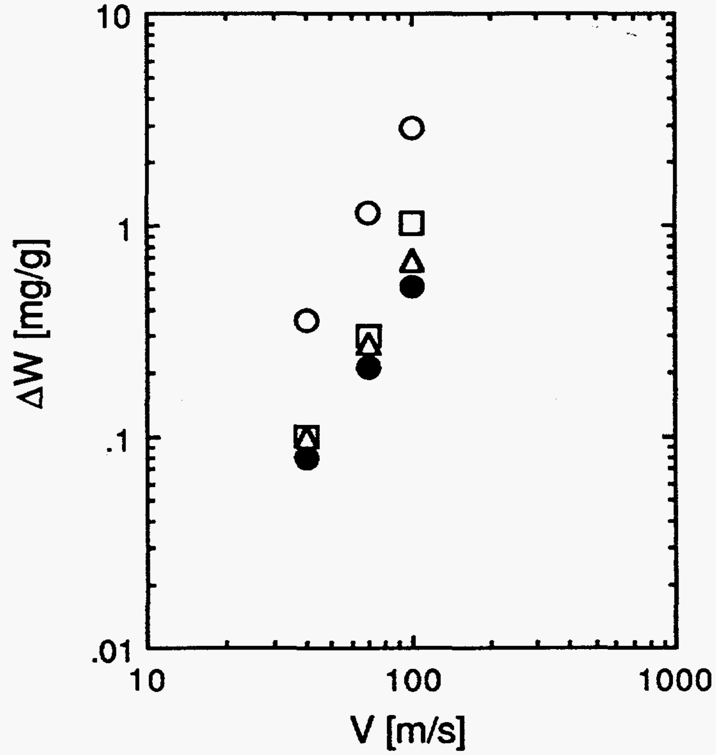

Figure 2. Steady-state erosion rates at normal incidence for a series of Al_2O_3-SiC(w) composites with 143–μm–diameter SiC erodents. Weight percent of whiskers of each composite is: open circles–0, open squares–5, open triangles–15, and solid circles–25.

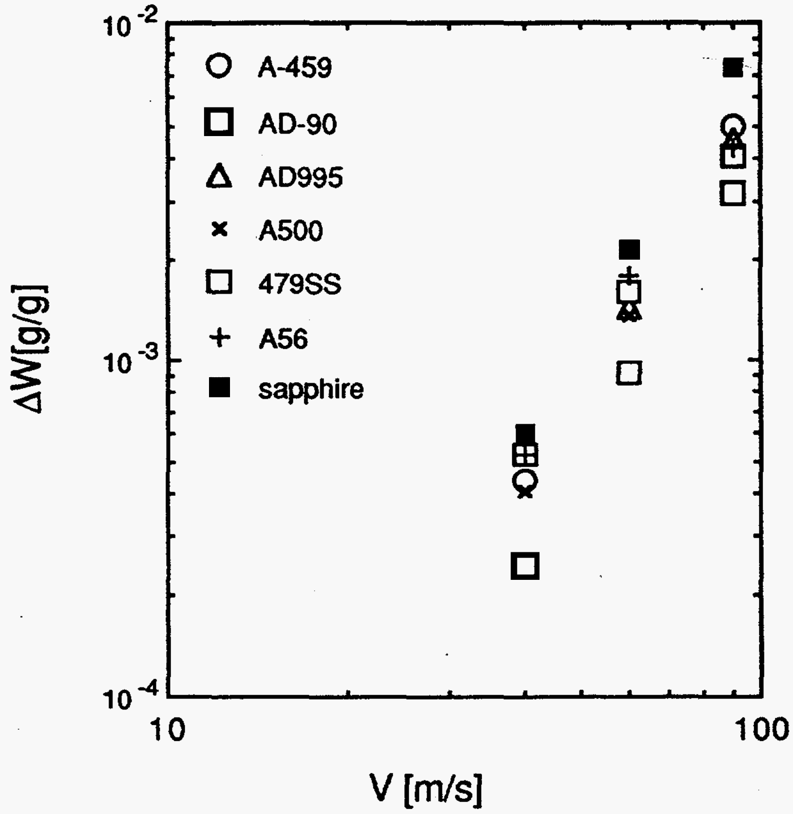

Figure 3. Steady-state erosion rates for various grades of alumina measured for 405–µm Al_2O_3 erodents impacting at normal incidence [21].

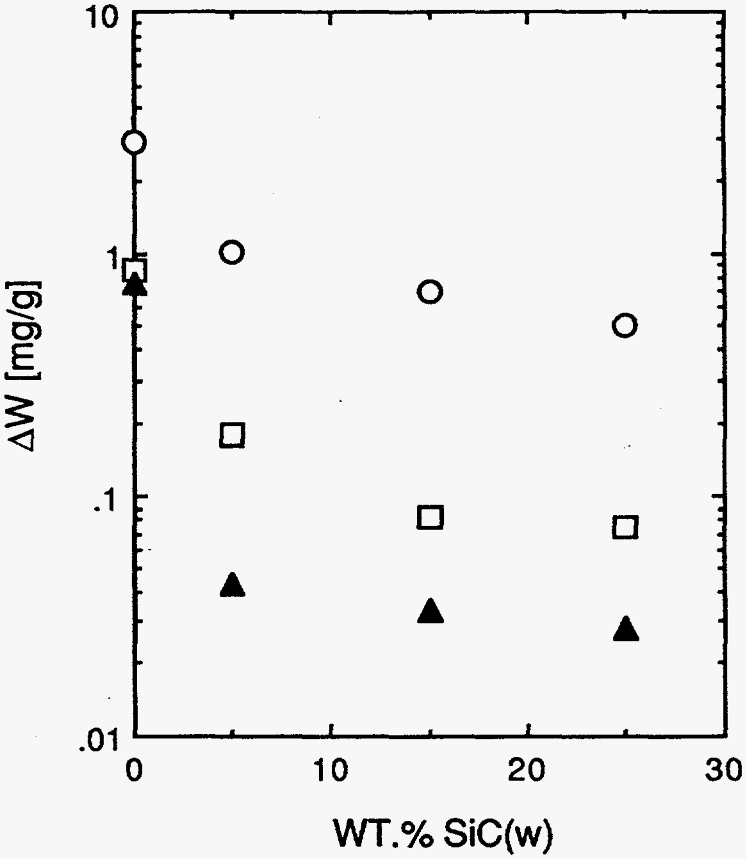

Figure 4. Steady-state erosion rate measured at normal incidence for impacting velocity of 100 m/s with 143–μm–diameter erodents of SiC (circles), Al_2O_3 (squares), and a 75% Al_2O_3 - 25% ZrO_2 abrasive (triangles).

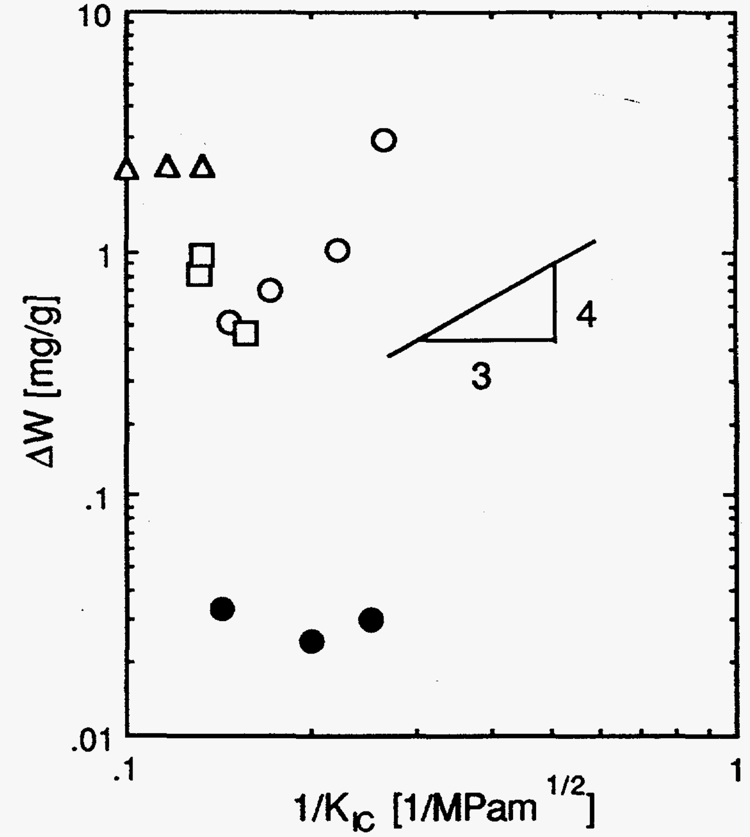

Figure 5. Steady-state erosion rate versus $1/K_{IC}$ for four whisker-reinforced composites measured with 143–µm–diameter SiC abrasives. Symbols are Si_3N_4 (squares), Al_2O_3–SiC(w) (open circles), Si_3N_4–SiC(w) (filled circles), and Y_2O_3–stabilized ZrO_2–Al_2O_3(w) (triangles).